Inertial-Range Reconnection in Magnetohydrodynamic Turbulence and in the Solar Wind

Cristian C. Lalescu,[1] Yi-Kang Shi,[1] Gregory L. Eyink,[1,2,*] Theodore D. Drivas,[1]
Ethan T. Vishniac,[3] and Alexander Lazarian[4]
[1]Department of Applied Mathematics and Statistics, The Johns Hopkins University, Baltimore, Maryland 21218, USA
[2]Department of Physics and Astronomy, The Johns Hopkins University, Baltimore, Maryland 21218, USA
[3]Department of Physics and Engineering Physics, University of Saskatchewan, Saskatoon, Saskatchewan S7N 5E2, Canada
[4]Department of Astronomy, University of Wisconsin, 475 North Charter Street, Madison, Wisconsin 53706, USA
(Received 1 March 2015; published 7 July 2015; corrected 10 July 2015)

In situ spacecraft data on the solar wind show events identified as magnetic reconnection with wide outflows and extended "*X* lines," 10^3–10^4 times ion scales. To understand the role of turbulence at these scales, we make a case study of an inertial-range reconnection event in a magnetohydrodynamic simulation. We observe stochastic wandering of field lines in space, breakdown of standard magnetic flux freezing due to Richardson dispersion, and a broadened reconnection zone containing many current sheets. The coarse-grain magnetic geometry is like large-scale reconnection in the solar wind, however, with a hyperbolic flux tube or apparent *X* line extending over integral length scales.

DOI: 10.1103/PhysRevLett.115.025001 PACS numbers: 52.30.Cv, 95.30.Qd, 96.50.Ci

Magnetic reconnection is widely theorized to be the source of explosive energy release in diverse astrophysical systems, including solar flares and coronal mass ejections [1], γ-ray bursts [2], and magnetar giant flares [3]. Because of the large length scales involved and consequent high Reynolds numbers, many of these phenomena are expected to occur in a turbulent environment, which profoundly alters the nature of reconnection [4–7]. In the solar wind near 1 A.U., which is the best-studied turbulent plasma in nature, quasistationary reconnection has been observed for magnetic structures at a large range of scales. In particular, reconnection outflow jets are reported with widths of order the ion gyroradius ($\sim$100 km) for microreconnection events, but also with widths up to integral length scales ($\sim 10^5$ km), and even wider outflows [8]. Yet numerical studies of reconnection in magnetohydrodynamic (MHD) turbulence simulations have focused almost exclusively on small-scale reconnection at thin current sheets with resistive-scale widths [9–12]. Our objective in this Letter is to identify a reconnection event with an inertial-range width in a MHD turbulence simulation and to determine its characteristic signatures, for comparison with observations in the solar wind and other turbulent astrophysical environments.

To search for reconnection zones of inertial-range width, we adapt standard observational criteria employed for the solar wind. In pioneering studies, Gosling [8] has looked for simultaneous large increments of magnetic field $\delta\mathbf{B}(\mathbf{r})$ and velocity field $\delta\mathbf{u}(\mathbf{r})$ across space separations r near the proton gyroradius ρ_p, which approximate MHD rotational discontinuities. Candidate reconnection events are then identified as pairs of such near discontinuities, with $\delta\mathbf{B}(\mathbf{r})$ aligned for the two members of the pair and $\delta\mathbf{u}(\mathbf{r})$ antialigned. Gosling's selected events generally have the appearance of two back-to-back shocks, or a "bifurcated current sheet." We modify this criterion to also allow for more gradual field reversals, by choosing instead $r = L/10$, with L the outer (integral) length of the turbulent inertial range, and by considering pairs separated by distances up to $L/2$.

We apply the above criterion to two data sets. The first is from a numerical simulation of incompressible, resistive MHD in a $[-\pi, \pi]^3$ periodic cube, in a state of stationary turbulence driven by a large-scale body force. The simulation has about a decade of power-law inertial range, and the full output for a large-scale eddy turnover time is archived in an online, Web-accessible database [13]. The second data set consists of *Wind* spacecraft observations of the solar wind magnetic field $\mathbf{B}$, velocity $\mathbf{u}$, and proton number density n_p. The results presented here are from a week-long fast stream in days 14–21 of 2008 (cf. Ref. [14]). The average solar wind conditions were $u = 638$ km/s, $B = 4.3$ nT, $n_p = 2.3$ cm^{-3}, Alfvén speed $V_A = 62$ km/s, proton beta $\beta_p = 1.1$, and proton gyroradius $\rho_p = 154$ km. The temporal data stream from the spacecraft is converted to an equivalent space series using Taylor's hypothesis, $x = ut$ [15]. Simulated spacecraft observations from the MHD database are taken along 192 linear cuts, with 8^2 cuts through each face of the simulation cube in the three coordinate directions. We find a good correspondence for statistics of $\delta\mathbf{B}(\mathbf{r})$ and $\delta\mathbf{u}(\mathbf{r})$ in the two data sets, with the grid spacing $dx = 2\pi/1024$ of the simulation related to 18 s of the *Wind* time series [16]. We thus estimate the turbulent outer scale L of the solar wind stream to be 6.5×10^5 km, or $\sim$1026 s in time units, which agrees well with the largest scale where the inertial-range scaling $|\delta\mathbf{B}(\mathbf{r})| \sim r^{1/3}$ holds well.

The corresponding length is $L = 0.35$ in the MHD simulation.

Increments $\delta\mathbf{B}(\mathbf{r}), \delta\mathbf{u}(\mathbf{r})$ are considered to be large for our criterion when their magnitudes both exceed 1.5 of their rms values. Using this threshold, we identify possible reconnection events in both data sets. See complete catalogs in Ref. [16]. Many of the candidate events in both data sets resemble the "double-step" magnetic reversals bounded by near discontinuities, which Gosling tends to select with his original criteria [8]. However, we also see events with more gradual reversals over inertial-range scales in both data sets. In Fig. 1 we show events of this latter type. The vectors have been rotated into the minimum-variance frame (MVF) of the magnetic field [17], calculated over the reversal region. The velocities here (and in all following plots) are in a frame moving with the local mean plasma velocity. Both events have inertial-range widths, occupying an interval of length 0.1 in the MHD simulation and 2–3 min in the solar wind case. Although they do not have a double-step magnetic structure, these two events do show the features characteristic of magnetic reconnection. There appears to be a reconnecting field component and an associated Alfvénic outflow jet in the L direction of maximum variance. A weak inflow is seen in the N direction of minimum variance, which is usually interpreted as across the reconnection current sheet. The M direction of intermediate variance is nominally the guide-field direction, which in both events appears rather weak and variable.

The MHD event shown in Fig. 1, top panels, arises from passage of the sampled 1D cut close to a large, helical magnetic flux rope appearing in the simulation. The maximum field strength in the rope is 8 times the rms strength in the database. Plotted in Fig. 2 is the original 1D spatial cut, the magnetic cloud, and nominally incoming and outgoing field lines along the N and L directions of the MVF. There is a clear magnetic reversal, with incoming lines in the flux rope twisting clockwise and into the page, but incoming lines to the left pointing out of the page. The field-line geometry is, however, quite complex since the lines exhibit the stochastic wandering assumed in the Lazarian-Vishniac theory of turbulent reconnection [5]. Figure 2 and all other spatial plots in this Letter are available as 3D PDFs [16] and were prepared with MayaVi [18].

To identify large-scale geometry, it is necessary to spatially coarse grain (low-pass filter) the magnetic field. For the theoretical basis of this coarse graining approach to turbulent reconnection, see Refs. [19,20]. Here we apply a box filter with half-width L to obtain coarse-grained fields $\bar{\mathbf{B}}$, $\bar{\mathbf{u}}$, from which all inertial- and dissipation-range eddies are eliminated. The nature of the database event as large-scale reconnection becomes more evident in Fig. 3, which plots the lines of $\bar{\mathbf{B}}$. A central "X point" at (2.84, 1.31, 5.73) was located by eye and a new MVF calculated in a sphere of radius L around that point. (This frame is rotated by ~20° in all three directions relative to the MVF for the original 1D cut, but furthermore, the M and N directions are exchanged.) Field lines are plotted at regular intervals along the L and N axes through the point. The plasma flow is incoming along the N direction and outgoing along the L direction, and the magnetic structure is clearly X type, with length ~0.4–0.6 (L direction) and width ~0.15–0.2 (N direction). Reconnection events observed in the solar wind also appear to be X type [8], although this structure

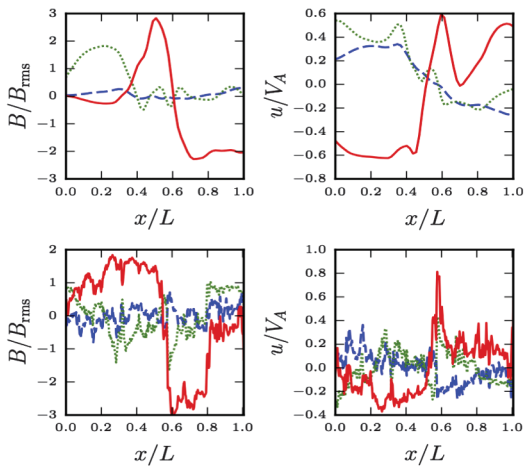

FIG. 1 (color). Top: Event from the MHD simulation, at point (2.964,0.908,5.841) along a cut in the y direction. Magnetic fields (left) normalized by $B_{\rm rms} = 0.24$, and velocity fields (right) by local upstream Alfven velocity $V_A = 0.7$. Bottom: Event from *Wind* spacecraft data, on January 14, 2008, 13:50 h, normalized by $B_{\rm rms} = 2.5$ nT, $V_A = 75$ km/s. Distance x is normalized by L. MVF components are identified as L (red solid line), M (green dotted line), N (blue dashed line).

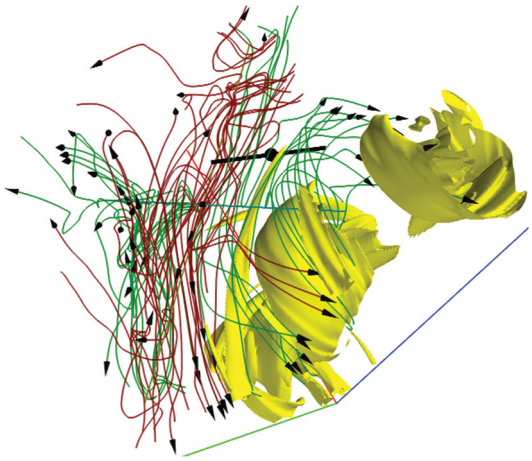

FIG. 2 (color). B isosurface at half maximum value 1.11 in yellow. $\mathbf{B}$ lines sampled along N direction in green and L direction in red. The original 1D spatial cut is the thick black line.

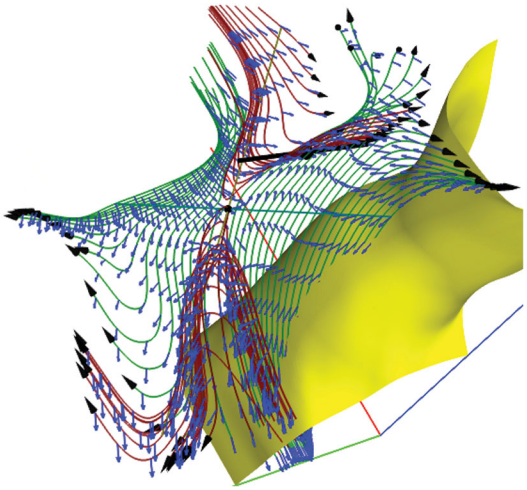

FIG. 3 (color). Same as Fig. 2, except for $\bar{\mathbf{B}}$ rather than $\mathbf{B}$. The isosurface is for the half maximum value $|\bar{\mathbf{B}}| = 0.301$. The blue vectors on the field lines are $\bar{\mathbf{u}}$ (in the local plasma frame).

has generally been interpreted in terms of Petschek reconnection.

In fact, the field-line geometry of $\bar{\mathbf{B}}$ in the MHD event is more complex than a single X point. The complete structure is revealed by calculating the perpendicular squashing factor $Q_\perp$, a quantity devised to identify field lines with rapidly changing connectivity in the solar photosphere and corona [21]. We consider the $Q_\perp$ factor for the field lines of $\bar{\mathbf{B}}$ which begin and end on a sphere of radius $1.6L$ around the nominal X point in Fig. 3. The $Q_\perp$ isosurface in Fig. 4 reveals a quasiseparatrix layer (QSL) whose cross section has a clear X-type structure. The hyperbolic flux tube (HFT) extending along the centers of these X's has length about 0.54 and is aligned approximately with the M direction, to within about 35°. A HFT is the modern version of an "X line" for 3D reconnection, which does not usually admit true separatrices and X lines, and a HFT has the same observational consequences as an X line. It is thus interesting that very large-scale reconnection events in the solar wind (above integral scales) appear to have very

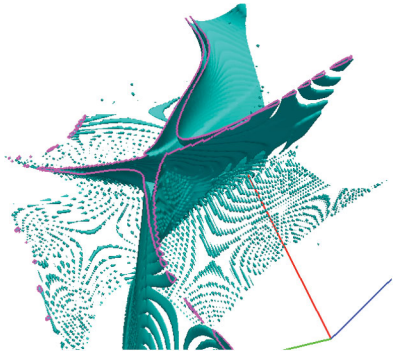

FIG. 4 (color). The quasiseparatrix layer $Q_\perp = 32$ in cyan, and its cross section in a plane normal to the M direction in magenta.

extended X lines, based on observations by multiple spacecraft [22].

Careful examination of the dynamics of this MHD event verifies that it is indeed magnetic reconnection, and fundamentally influenced by turbulence. The magnetic flux rope and the associated QSL persist over the entire time (0–2.56) of the database, drifting slowly with the plasma. The QSL and MVF also slowly rotate in time, with the MVF directions rotated through total angles ~40° at the final time and also the M and N directions exchanged around time 2.0. The time required for a plasma fluid element in the reconnection region to be carried out by the exhausts with velocities ~0.3–0.4 also happens to be about 2.0. Despite the high conductivity of the simulation, standard flux freezing is violated in this event due to the turbulent phenomenon of spontaneous stochasticity, as we now verify. The exact stochastic flux-freezing theorem for resistive MHD [23] (which generalizes ordinary flux freezing) states that field lines of the fine-grained magnetic field $\mathbf{B}$ are "frozen in" to the stochastic trajectories solving the Langevin equation

$$d\mathbf{x}/dt = \mathbf{u}(\mathbf{x}, t) + \sqrt{2\lambda}d\boldsymbol{\eta}(t), \tag{1}$$

where $\lambda = \eta c^2/4\pi$ is magnetic diffusivity and $\boldsymbol{\eta}(t)$ is a 3D Gaussian white noise. The many virtual field vectors $\tilde{\mathbf{B}}$ that arrive to the same final point must be averaged to obtain the physical magnetic field $\mathbf{B}$ at that point. We have chosen a point $\mathbf{x}_f$ in the outflow jet in the $+L$ direction at time $t_f = 2$ and solved Eq. (1) backward in time to $t_0 = 0$, to find the positions of the initial points whose magnetic field

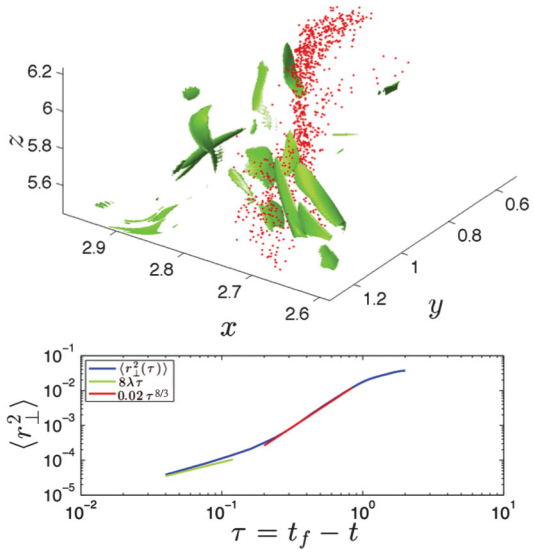

FIG. 5 (color). Top: Current isosurfaces at the half maximum value $j = 69.1$ in green. In red, origin points at time $t = 0$ of magnetic field at final point $(\mathbf{x}_f, t_f) = (3.31, 0.083, 6.07, 2.00)$. Bottom: Backward mean-square dispersion $\langle r_\perp^2(\tau) \rangle$ orthogonal to L direction as blue line. Reference curve $\langle r_\perp^2 \rangle = 8\lambda\tau$ in green and $\langle r_\perp^2 \rangle = 0.02\tau^{8/3}$ in red.

vectors arrive at $(\mathbf{x}_f, t_f)$. This ensemble of points, plotted in Fig. 5, is widely dispersed in space. This disagrees with the predictions of standard flux freezing, which implies that the ensemble should be close to a single point. In the lower panel of Fig. 5 we plot the mean-square dispersion of this ensemble perpendicular to the L direction, $\langle r_\perp^2 \rangle$, as a function of reversed time $\tau = t_f - t$. Consistent with previous results [7], the (backward) growth of perpendicular dispersion is diffusive $\langle r_\perp^2(\tau) \rangle \sim 8\lambda\tau$ for very small τ but then becomes superballistic, due to turbulent Richardson dispersion. Unlike in Ref. [7], which averaged over points $\mathbf{x}_f$ distributed homogeneously in space, the present results are for a single point in the outflow, thus demonstrating that such superballistic dispersion occurs within a turbulent reconnection zone. As argued in Ref. [6], the perpendicular spread in the time to exit with the outflow, $\sqrt{\langle r_\perp^2(2) \rangle} \sim 0.19$, is close to the width of the reconnection region. This zone has both the width and the turbulent structure proposed in Ref. [5], as can also be seen in Fig. 5 which plots in green the isosurfaces of the fine-grained current magnitude at half maximum. There is a spatial distribution of many current sheets rather than a single large current sheet, as in laminar reconnection, and none of the sheets is located precisely at the QSL shown in Fig. 4. See Ref. [16] for 3D plots. As in previous studies of current sheets in homogeneous MHD turbulence [9–12], we find that these sheets are "ribbonlike," with widths (roughly the N direction) typically of order the Kolmogorov length 0.003, lengths in roughly the L direction of order 1–3 integral lengths, and heights in the third direction ranging from the Taylor length 0.06 to the integral length 0.35. However, as we document below, these intense current sheets do not play a dominant role in the inertial-range turbulent reconnection process.

The breakdown of standard flux freezing is one evidence of reconnection in this event [24]. We have also verified that there is topology change of the lines of both fine-grained and coarse-grained magnetic fields. To show this, we decorate initial field lines of either $\mathbf{B}$ or $\bar{\mathbf{B}}$ at time $t = 0$ with a sequence of plasma fluid elements and then follow each element moving with the local velocity $\mathbf{u}$ forward in time to $t = 2$. We find that the plasma elements that initially resided on the same line at $t = 0$ end up on distinct lines at time $t = 2$, and some of these lines are outgoing in the $+L$ direction and others in the $-L$ direction. For movies, see Ref. [16]. The videos in Ref. [16] also show that the reconnection of individual field lines is not dependent upon the intense current sheets, with lines well away from the strong sheets both slipping relative to the plasma and undergoing topology change. To understand this observation, recall that breaking the frozen-in property of field lines does not require a large value of Ohmic electric field $\eta\mathbf{J}$ but instead a non-negligible value of $\hat{\mathbf{B}} \times (\nabla \times \eta\mathbf{J})$ [25]. It has been shown that $\Sigma = \hat{\mathbf{B}} \times [\hat{\mathbf{B}} \times (\nabla \times \eta\mathbf{J})]/|\mathbf{B}|$ gives the slippage velocity of field lines relative to the plasma fluid which is developed per unit arclength of line [20]. For a field line to achieve a slip velocity equal to the rms plasma velocity ~0.23 over an integral length ~0.35 of field line requires a magnitude of only $|\Sigma| \sim 0.66$, and such values occur ubiquitously throughout the turbulent flow, not only at intense current sheets. See Ref. [16] for a 3D plot of the isosurface $|\Sigma| = 0.66$. These data are further evidence that the usual frozen-in property fails everywhere in turbulent MHD flow.

We have also determined the average reconnecting electric field $E_{\rm rec}$ for the large-scale magnetic field $\bar{\mathbf{B}}$, using a voltage measure proposed in Ref. [26]. We find that $E_{\rm rec} \sim 0.01 v_A B$ in terms of local upstream values v_A and B. Furthermore, at the length scale L of $\bar{\mathbf{B}}$, most of $E_{\rm rec}$ is supplied by turbulence-induced electric fields, and resistivity gives only a tiny contribution, always more than an order of magnitude smaller. These and many other detailed results for this event will be presented elsewhere. One finding is that this inertial-range event is not only highly 3D but also nonstationary in time. While the outflow jets are quite stable over time, the inflow is "gusty," with variable magnitude and direction veering in the $N - M$ plane (so that it is often in the nominal guide-field or M direction). It is thus difficult to define an operationally meaningful reconnection speed.

The main purpose of this Letter has been to present an example of inertial-range reconnection in MHD turbulence, to clarify its observational signatures. While a fluid description is surely applicable only to scales much larger than plasma microscales (e.g., the ion gyroradius in the collisionless solar wind), our simulation is remarkably successful in reproducing observed features of large-scale solar wind reconnection, together with crucial turbulent effects supporting theoretical predictions in Refs. [5,6]. Our results also suggest that current observational studies in the solar wind [8] are employing too narrow search criteria that may miss much inertial-range reconnection. For example, Gosling's original criterion with increments $\delta\mathbf{B}(\mathbf{r}), \delta\mathbf{u}(\mathbf{r})$ required to be large over ion-scale separations r would miss a solar wind event like that pictured in Fig. 1, bottom panels, where these increments are achieved more gradually over inertial-range separations r. The comparison with our MHD simulation event makes it very plausible that the solar wind data in Fig. 1 represent inertial-range turbulent reconnection.

The characteristics of reconnection are expected to change with length scale; e.g., deeper within the inertial range there should be stronger guide fields or smaller magnetic shear angles [5,27]. We also note some differences between the current MHD database and the solar wind, as our simulation is incompressible and isothermal, whereas the solar wind is slightly compressible and reconnection events there (including that in Fig. 1) often show enhancements of proton density and

temperature in the reconnection zone. Furthermore, our MHD simulation has no mean magnetic field and is close to balance between Alfvén wave packets (described by Elsasser fields) propagating parallel and antiparallel to field lines, whereas the solar wind has a moderate mean field and the high-speed stream studied in this work is dominated by Alfvén waves propagating outward from the Sun. The influence of these differences should be explored in future work seeking to explain large-scale solar wind reconnection in detail within a MHD turbulence framework.

This work was supported by NSF Grants No. CDI-II: CMMI 0941530 and No. AST 1212096.

*eyink@jhu.edu

[1] E. Priest and T. Forbes, *Magnetic Reconnection: MHD Theory and Applications* (Cambridge University Press, Cambridge, UK, 2007).
[2] B. Zhang and H. Yan, The internal-collision-induced magnetic reconnection and turbulence (ICMART) model of gamma-ray bursts, Astrophys. J. **726**, 90 (2011).
[3] M. Lyutikov, Magnetar giant flares and afterglows as relativistic magnetized explosions, Mon. Not. R. Astron. Soc. **367**, 1594 (2006).
[4] W. H. Matthaeus and S. L. Lamkin, Turbulent magnetic reconnection, Phys. Fluids **29**, 2513 (1986).
[5] A. Lazarian and E. Vishniac, Reconnection in a weakly stochastic field, Astrophys. J. **517**, 700 (1999).
[6] G. L. Eyink, A. L. Lazarian, and E. T. Vishniac, Fast magnetic reconnection and spontaneous stochasticity, Astrophys. J. **743**, 51 (2011).
[7] G. Eyink, E. Vishniac, C. Lalescu, H. Aluie, K. Kanov, K. Bürger, R. Burns, C. Meneveau, and A. Szalay, Flux-freezing breakdown in high-conductivity magnetohydrodynamic turbulence, Nature (London) **497**, 466 (2013).
[8] J. T. Gosling, Magnetic reconnection in the solar wind, Space Sci. Rev. **172**, 187 (2012).
[9] S. Servidio, W. H. Matthaeus, M. A. Shay, P. Dmitruk, P. A. Cassak, and M. Wan, Statistics of magnetic reconnection in two-dimensional magnetohydrodynamic turbulence, Phys. Plasmas **17**, 032315 (2010).
[10] V. Zhdankin, D. A. Uzdensky, J. C. Perez, and S. Boldyrev, Statistical analysis of current sheets in three-dimensional magnetohydrodynamic turbulence, Astrophys. J. **771**, 124 (2013).
[11] K. T. Osman, W. H. Matthaeus, J. T. Gosling, A. Greco, S. Servidio, B. Hnat, S. C. Chapman, and T. D. Phan, Magnetic Reconnection and Intermittent Turbulence in the Solar Wind, Phys. Rev. Lett. **112**, 215002 (2014).
[12] M. Wan, A. F. Rappazzo, W. H. Matthaeus, S. Servidio, and S. Oughton, Dissipation and reconnection in boundary-driven reduced magnetohydrodynamics, Astrophys. J. **797**, 63 (2014).
[13] Johns Hopkins Turbulence Databases, http://turbulence.pha.jhu.edu.
[14] J. T. Gosling, Observations of magnetic reconnection in the turbulent high-speed solar wind, Astrophys. J. Lett. **671**, L73 (2007).
[15] G. I. Taylor, The spectrum of turbulence, Proc. R. Soc. A **164**, 476 (1938).
[16] See Supplemental Material at http://link.aps.org/supplemental/10.1103/PhysRevLett.115.025001 for 3D figures, movies, and additional documentation of the procedures.
[17] B. U. O. Sonnerup and L. J. Cahill, Jr., Magnetopause structure and attitude from Explorer 12 observations, J. Geophys. Res. **72**, 171 (1967).
[18] P. Ramachandra and G. Varoquaux, MayaVi: 3D visualization of scientific data, IEEE Comput. Sci. Eng. **13**, 40 (2011).
[19] G. L. Eyink and H. Aluie, The breakdown of Alfvén's theorem in ideal plasma flows: Necessary conditions and physical conjectures, Physica (Amsterdam) **223D**, 82 (2006).
[20] G. L. Eyink, Turbulent general magnetic reconnection, arXiv:1412.2254 [Astrophys. J. (to be published)].
[21] V. S. Titov, Generalized squashing factors for covariant description of magnetic connectivity in the solar corona, Astrophys. J. **660**, 863 (2007).
[22] T. D. Phan, J. T. Gosling, and M. S. Davis, Prevalence of extended reconnection *X*-lines in the solar wind at 1 AU, Geophys. Res. Lett. **36**, L09108 (2009).
[23] G. L. Eyink, Stochastic line motion and stochastic flux conservation for nonideal hydromagnetic models, J. Math. Phys. **50**, 083102 (2009).
[24] J. M. Greene, Reconnection of vorticity lines and magnetic lines, Phys. Fluids B **5**, 2355 (1993).
[25] W. A. Newcomb, Motion of magnetic lines of force, Ann. Phys. (N.Y.) **3**, 347 (1958).
[26] G. Kowal, A. Lazarian, E. T. Vishniac, and K. Otmianowska-Mazur, Numerical tests of fast reconnection in weakly stochastic magnetic fields, Astrophys. J. **700**, 63 (2009).
[27] J. T. Gosling, T. D. Phan, R. P. Lin, and A. Szabo, Prevalence of magnetic reconnection at small field shear angles in the solar wind, Geophys. Res. Lett. **34**, L15110 (2007).